INTERNATIONAL JOURNAL OF ROBUST AND NONLINEAR CONTROL
Int. J. Robust. Nonlinear Control 2014; **24**:2724–2740
Published online 22 May 2013 in Wiley Online Library (wileyonlinelibrary.com). DOI: 10.1002/rnc.3020

FTC approach with actuator saturation avoidance based on reference management

Boumedyen Boussaid[1,3,*,†], Christophe Aubrun[1], Jin Jiang[2] and Mohamed Naceur Abdelkrim[3]

[1]*Université de Lorraine, CRAN, UMR 7039, Campus Sciences, BP 70239, Vandœuvre-lès-Nancy Cedex, 54506, France*
[2]*Department of Electrical & Computer Engineering, University of Western Ontario, London, ONT. N6A 5B9, Canada*
[3]*MACS Research Unit, ENIG School, University of Gabes, Omar Ibn Khattab road, 6029 Gabes, Tunisia*

SUMMARY

In this paper, a fault recovery approach using dynamic reference modification and reconfigurable linear quadratic regulator is proposed. The idea is to modify the reference according to the system constraints, which become more strict after fault occurrence to avoid any actuator saturation and ensure system stability. The effectiveness of the proposed method is evaluated by a performance index based on tracking reference error and illustrated by an aircraft example subject to actuator faults and constrained on the actuator dynamic ranges. Copyright © 2013 John Wiley & Sons, Ltd.

Received 25 October 2012; Revised 1 March 2013; Accepted 2 April 2013

KEY WORDS: fault tolerant control; performance degradation; reference management; actuator saturation; performance index

1. INTRODUCTION

In industrial processes, systems to be controlled are becoming more and more complex. One of these complexities relies in the necessity of satisfying input/state constraints, which are dictated by physical limitations of the actuators and by the necessity to keep some plant variables within safe limits. In general, these constraints are integrated in the selection of the process equipment and the design of the nominal controllers. Another complexity is the occurrence of faults in plants, which make the design of a controller tolerant to faults a very important issue. Several excellent survey papers have been carried out in fault-tolerant control (FTC) framework [1–5].

For an FTC design, the post-fault system should recover the original performance, which is usually a quiet ambitious objective. In [6] and [7], it is considered that the system can always operate under degraded performance. In practice, once a fault occurs, the degree of the system redundancy and the available actuator capabilities can be significantly reduced. Further, the FTC may lead to actuator saturation, or worse still, may cause damage to the system and even result in lose of the system stability [8].

A significant amount of work has been carried out to deal with actuator saturation. Model predictive control is an effective control algorithm for dealing with actuator saturation [9]. Anti-windup research was largely discussed, and many constructive design algorithms were formally proved to induce suitable stability properties [10, 11]. Other class of framework consists of modifying the reference input so that the constraints are not violated [12–17]. These approaches are able to

*Correspondence to: Boumedyen Boussaid, Department of Automatic Control, National Engineering School of Gabes, University of Gabes, 6029 Gabes, Tunisia.

†E-mail: boumedyen.boussaid@gmail.com

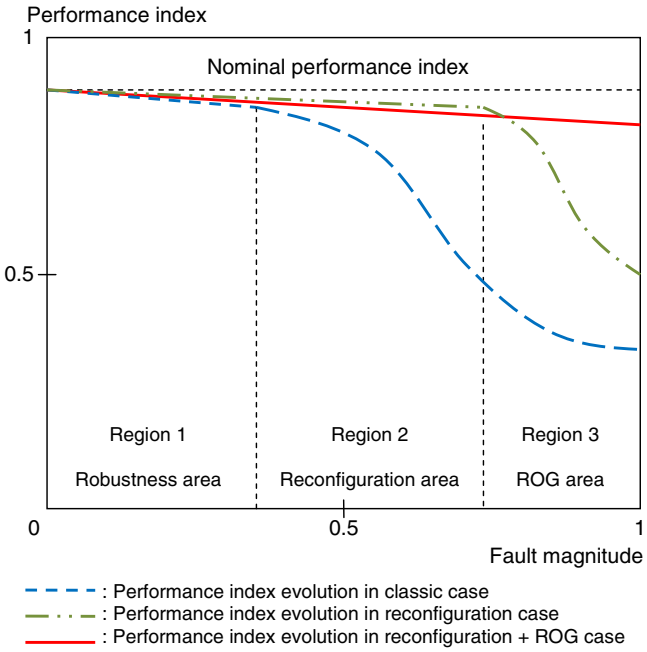

Figure 1. Performance degradation versus fault magnitude. ROG, reference-offset governor.

handle input and/or state-related constraints, using methods based on model predictive control ideas, to synthesize command or reference governor (RG). In [18], parameter governor (PG) unit is proposed, which enforces pointwise-in-time constraints on the evolutions of relevant system variables. Later, both RG and PG actions are integrated in a single unit as reference-offset governor (ROG) [19], which adds many advantages especially in enlarging the set of feasible evolutions of the system. The function of ROG device is to modify, whenever necessary, the reference and add an offset to the nominal control action to enforce pointwise-in-time constraints and to improve the overall system transient performance [19, 20].

In this paper, a new reconfiguration system approach based on ROG and separate LQ controller is proposed. The reconfiguration capability of ROG unit is basically the respect of system constraint obligations and the dynamic modification of the reference according to an acceptable performance degradation. Furthermore, the stability of the closed-loop system is ensured, and the performance degradation is controlled by a performance index designed to evaluate the global system.

The concept of gradual action of control law in terms of the fault severity is illustrated in Figure 1. According to the severity of the fault, three regions could be formed. For region 1, the intrinsic robustness propriety of the nominal controller can compensate the effect of minor faults. In region 2, one should modify the control law to compensate the fault effect, which corresponds to reconfiguration action. In region 3, and for high severity of fault, one should modify indeed the control objectives, which corresponds to performance degradation.

The main contribution of this paper is to deal with performance degradation in the case of constrained control system subject to actuator faults. A nonlinear reference management is used to ensure actuator-saturation avoidance and system stability with acceptable performance degradation via dynamic reference modification.

The paper is organized as follows. The reconfigurable LQ controller and its limitation in constrained control are presented in Section 2. Section 3 is dedicated to deal with dynamic reference management and especially the design of ROG device. In Section 4, the proposed FTC solution with reconfigurable action on LQ controller and ROG action is detailed. Section 5 is dedicated to illustrate the idea with an example of flight control followed by simulation results. Finally, the paper is ended by a conclusion.

DOI: 10.1002/rnc

2. LINEAR QUADRATIC REGULATOR IN CONSTRAINED CONTROL

2.1. LQ control in fault-free case

Let us consider the following linear time-invariant (LTI) system

$$\begin{cases} x(t+1) = Ax(t) + Bu(t) \\ y(t) = Cx(t) \end{cases} \tag{1}$$

where $x(k) \in \mathcal{R}^n$ is the state variable, $u(k) \in \mathcal{R}^m$ is the input vector, $y(k) \in \mathcal{R}^p$ is the output vector, and the pair (A,B) is stabilizable where (A,B,C) represents the system model in discrete time.

Let $rank(C) = p$, and $rank(B) = m \geqslant p$. Assume that the full-state x is available. By solving the linear quadratic regulation problem, the optimal control law ([21]) is given by

$$u(t) = -Kx(t) + K_r r(t) \tag{2}$$

with

$$K = R^{-1}B^T P \tag{3}$$

$$K_r = R^{-\frac{1}{2}}(C(BK - A)^{-1}BR^{-\frac{1}{2}})^+ \tag{4}$$

where $r(t) \in \mathcal{R}^p$ is the nominal reference, Q is a positive semi-definite matrix, and R is a positive definite matrix. Q and R are preselected by the designer to achieve the nominal performance. P is a unique positive semi-definite and symmetric solution of the algebraic Riccati equation

$$A^T P + PA + Q - PBR^{-1}B^T P = 0 \tag{5}$$

2.2. LQ control in post-fault case

Assume that, after fault occurrence, the new dynamics can be expressed as

$$\begin{cases} x(t+1) = A_f x(t) + B_f u(t) \\ y(t) = Cx(t) \end{cases} \tag{6}$$

where the matrices A_f and B_f are detectable and the post-fault system is controllable. By assuming that (A_f,B_f) is still stabilizable and from the Bellman's optimality principle, the optimal reconfigurable strategy ([22]) consists of applying a new optimal control to system (6):

$$u_f(t) = -K_f x(t) + K_r^f r(t) \tag{7}$$

with

$$K_f = R^{-1}B_f^T P_f \tag{8}$$

$$K_r^f = R^{-\frac{1}{2}}(C(B_f K_f - A_f)^{-1}B_f R^{-\frac{1}{2}})^+ \tag{9}$$

where P_f is a unique positive semi-definite and symmetric solution of the algebraic Riccati equation

$$A_f^T P_f + P_f A_f + Q - P_f B_f R^{-1}B_f^T P_f = 0 \tag{10}$$

2.3. Limitation of the LQ solution in constrained control

Assume that one has constraints on the control signal, so one should use a block to limit the input signal to the upper and lower saturation values (Figure 2).

The new control signal with the consideration of a piecewise-linear saturation is described as

$$u_{j,s} = \sigma_j(u_j) = \begin{cases} u_{j,\max} & \text{if } u_j \geq u_{j,\max} \\ u_j & \text{if } u_{j,\min} \leq u_j \leq u_{j,\max} \\ u_{j,\min} & \text{if } u_j \leq u_{j,\min} \end{cases} \quad for \quad j = 1,2,\ldots,m \tag{11}$$

DOI: 10.1002/rnc

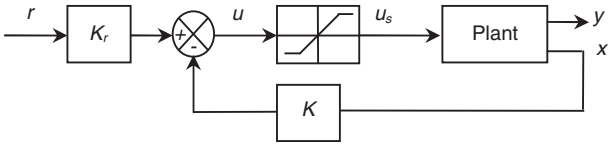

Figure 2. LQ regulator with input-signal limitation block.

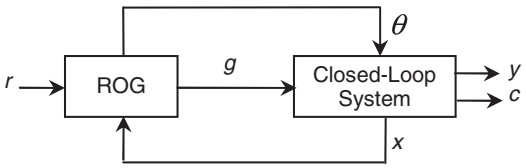

Figure 3. Reference-offset governor (ROG) principle.

where m is the number of actuators. $u_{j,\min}$ and $u_{j,\max}$ are the control saturation values, which depend on the actuator technology used in the power interface.

Ideally, the nominal LQ controller is designed to work inside the allowed control limit. However, a slight saturation is possible during a short time without destabilizing the system. In faulty case, these constraints become more strict, and the probability to reach the saturation region increases with the fault severity especially in the case of loss of actuator effectiveness, which may destabilize the system or induce severe performance degradation through a decrease of feedback gain [23].

In general, nonlinear control laws are required to stabilize linear systems subject to input saturation and, for more generality, subject to input/state constraints. The model predictive control is an effective control algorithm for dealing with actuator saturation [9]. Anti-windup research was largely discussed, and many constructive design algorithms were formally proved to induce suitable stability properties [10, 11].

Our approach consists of associating a reconfigurable ROG block to a reconfigurable LQ regulator to solve the problem of actuator saturations and input/state constraints in general. Besides, the performance degradation is taken account by modifying the references by the ROG unit with the consideration of system constraints and nominal objectives.

3. REFERENCE MANAGEMENT: REFERENCE-OFFSET GOVERNOR DESIGN

The ROG design is treated with details in [19]. The ROG unit is an add-on control device whose action is computed as a function of the actual reference $r(t)$, current state $x(t)$, and prescribed constraints $c(t)$. An ROG control scheme, with a plant in closed-loop and ROG device, is depicted in Figure 3.

Consider the following linear, time-invariant system of the plant in a closed-loop scheme:

$$\begin{cases} x(t+1) = \Phi x(t) + G_g g(t) + G_\theta \theta(t) + G_d d(t) \\ y(t) = H_y x(t) \\ c(t) = H_c x(t) + L_g g(t) + L_\theta \theta(t) + L_d d(t) \end{cases} \tag{12}$$

where $x(t) \in \mathcal{R}^n$ is the state vector; $r(t) \in \mathcal{R}^p$ the nominal reference; $g(t) \in \mathcal{R}^p$ the manipulable reference; $\theta(t) \in \mathcal{R}^m$ an adjustable offset on the nominal control law; $d(t) \in \mathcal{R}^{n_d}$ an exogenous bounded disturbance satisfying $d(t) \in \mathcal{D}$; $\forall t \in \mathcal{Z}_+$ with $\mathcal{D}$ a specified convex and compact set such that $0_{n_d} \in \mathcal{D}$ and n_d is the number of elements in vector $d(t)$; $y(t) \in \mathcal{R}^p$ the output, namely, a performance-related signal; $c(t) \in \mathcal{R}^{n_c}$ the constraint vector, $c(t) \in \mathcal{C}$; $\forall t \in \mathcal{Z}_+$, with $\mathcal{C} \subset \mathcal{R}^{n_c}$ a prescribed constrained set, and n_c is the number of elements in vector $c(t)$. Indeed, it is assumed that

A.1 Φ is a stable matrix;
A.2 The system (12) is offset free with respect to $g(t)$, that is, $H_y(I_n - \Phi)^{-1} G_g = I_p$.

DOI: 10.1002/rnc

Let us consider the following state-space description of (12).

$$\begin{cases} x(t+1) = \Phi x(t) + Gz(t) + G_d d(t) \\ y(t) = H_y x(t) \\ c(t) = H_c x(t) + Lz(t) + L_d d(t) \end{cases} \tag{13}$$

where $z(t) = [g(t)\theta(t)]^T \in \mathcal{R}^{p+m}$ is the ROG output and the following matrices are defined as $G = [G_g G_\theta]$, $L = [L_g \;\; L_\theta]$.
The ROG design problem consists of generating a command input $z(t)$ as a function of the current state $x(t)$ and reference $r(t)$

$$z(t) := \bar{z}(x(t), r(t)) \tag{14}$$

Adopting the following notations for the disturbance-free solutions of (13) to a constant command $z(t) = z$, we define

$$\begin{aligned} \bar{x}_z &:= (I_n - \Phi)^{-1} Gz \\ \bar{y}_z &:= H_y (I_n - \Phi)^{-1} Gz \\ \bar{c}_z &:= H_c (I_n - \Phi)^{-1} Gz + Lz \end{aligned} \tag{15}$$

Let one consider the following set recursion.

$$\begin{aligned} \mathcal{C}_0 &:= \mathcal{C} \sim L_d \mathcal{D} \\ \mathcal{C}_k &:= \mathcal{C}_{k-1} \sim H_c \Phi^{k-1} G_d \mathcal{D} \\ &\vdots \\ \mathcal{C}_\infty &:= \bigcap \mathcal{C}_k \end{aligned} \tag{16}$$

where $\mathcal{A} \sim \mathcal{E}$ is defined as $\{a \in \mathcal{A} : a + e \in \mathcal{A}, \forall e \in \mathcal{E}\}$. It can be shown that $\bar{c}(t) \in \mathcal{C}_\infty, \forall t \in \mathcal{Z}_+$ implies that $c(t) \in \mathcal{C}, \forall t \in \mathcal{Z}_+$. Thus, one can consider only disturbance-free evolutions of the system and adopt a 'worst-case' approach. In [13], two sets, for a given $\delta > 0$, are defined:

$$\mathcal{C}^\delta := \mathcal{C}_\infty \sim \mathcal{B}_\delta \tag{17}$$

$$\mathcal{W}_\delta := \left\{ z \in \mathcal{R}^{p+m} : \bar{c}_z \in \mathcal{C}^\delta \right\} \tag{18}$$

where $\mathcal{B}_\delta$ is a ball of radius δ centered at the origin and $\mathcal{W}_\delta$ is the set of all commands whose corresponding steady-state solution satisfies the constraints with margin δ.

The main idea is to choose at each time step a constant virtual command $z(\cdot) \equiv z$, with $z \in \mathcal{B}_\delta$ such that the corresponding virtual evolution fulfills the constraints over a semi-definite horizon. Moreover, it is required that the offset on the control law and the distance between the modified reference $g(t)$ and the nominal reference $r(t)$ are minimal. Let us define the set $\mathcal{V}(x(t))$ as

$$\mathcal{V}(x(t)) = \{ z \in \mathcal{W}_\delta : \bar{c}(k, x(t), z) \in \mathcal{C}_k, \forall k \in \mathcal{Z}_+ \} \tag{19}$$

where

$$\bar{c}(k, x(t), z) = H_c \left(\Phi^k x(t) + \sum_{i=0}^{k-1} \Phi^{k-i-1} Gz \right) + Lz \tag{20}$$

is to be understood as the disturbance-free virtual evolution at time k of the constraint vector from the initial condition $x(t)$ at time zero under the constant command $z(\cdot) \equiv z$:. As a consequence, $\mathcal{V}(x(t)) \subset \mathcal{W}_\delta$, and, if non-empty, it represents the set of all constant virtual sequences in $\mathcal{W}_\delta$ whose evolutions starting from $x(t)$ satisfy the constraints also during transients. It can also be shown that such a set is finitely determined, namely, there exists a positive integer k_0 such that (19) is identically characterizable by restricting $k \in \{0, \cdots, k_0\}$, with k_0 computable off-line as described in [17].

DOI: 10.1002/rnc

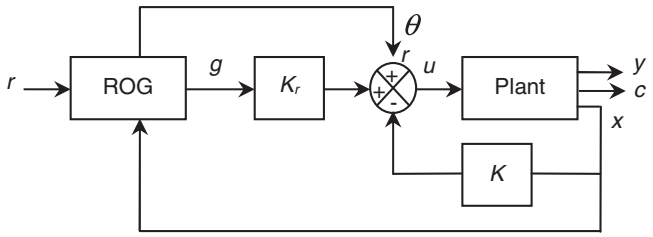

Figure 4. Block diagram of the system with reference-offset governor (ROG) unit.

The ROG output is based on the minimization of a cost function subject to the constraints imposed by (19). The cost function has the following form:

$$J(z(t), r) = \|g(t) - r\|^2_{\Psi_g} + \|\theta(t)\|^2_{\Psi_\theta} \tag{21}$$

where $\Psi_g = \Psi_g^T > 0_m$, $\Psi_\theta = \Psi_\theta^T > 0_m$, and $\|v\|^2_\Psi := v^T \Psi v$. Equation (21) expresses that the objective of RG is to determine $g(t)$ as close as possible to $r(t)$ to limit the degradation of the performances due to the occurrence of the fault. Thus, at each time $t \in \mathcal{Z}_+$, the ROG output is chosen according to the solution of the following constrained optimization problem.

$$z(t) := arg \min_{z \in \mathcal{V}(x(t))} J(z(t), r) \tag{22}$$

4. OVERALL STRUCTURE OF THE FAULT-TOLERANT CONTROL SCHEME

4.1. Global system diagram description

Let us consider the global system including the ROG unit and the LQ controller, as depicted in 'Figure 4'.

The control input is

$$\begin{aligned} u(t) &= K_r g(t) + \theta(t) - Kx(t) \\ &= K_z z(t) - Kx(t) \end{aligned} \tag{23}$$

where $K_z = [K_r \quad I_m]$ and $z(t) = [g(t) \quad \theta(t)]^T$.

One replaces (23) in (1), and one obtains

$$\begin{aligned} x(t+1) &= (A - BK)x(t) + BK_z z(t) + G_d d(t) \\ &= \Phi x(t) + Gz(t) + G_d d(t) \end{aligned} \tag{24}$$

where $\Phi = (A - BK)$ and $G = BK_z$.

Besides, if one considers only the control input constraints and one puts $H_c = -K$ and $L = K_z$,

$$c(t) = H_c x(t) + Lz(t) + L_d d(t) \tag{25}$$

So, the LTI system in (1) becomes

$$\begin{cases} x(t+1) = \Phi x(t) + Gz(t) + G_d d(t) \\ y(t) = H_y x(t) \\ c(t) = H_c x(t) + Lz(t) + L_d d(t) \end{cases} \tag{26}$$

4.2. Post-fault system description

In the faulty case, one supposes that the matrices A_f and B_f are detectable and the system after fault is controllable. One considers hereafter only the actuator faults, $A_f = A$ and $B_f = B(I_m - \Gamma)$, where Γ is the fault distribution matrix

$$\Gamma = diag(\gamma_i) \tag{27}$$

DOI: 10.1002/rnc

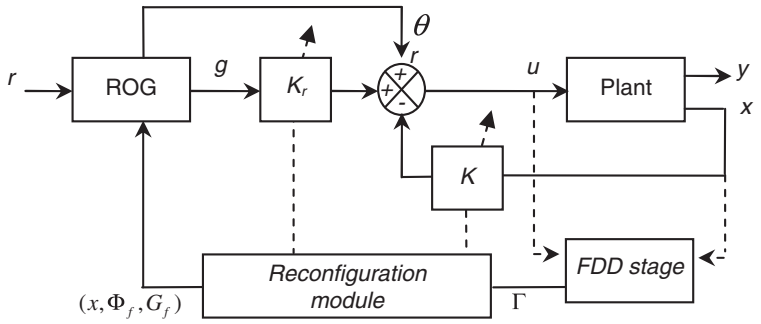

Figure 5. Block diagram of the fault-tolerant control scheme. FDD, fault detection and diagnosis; ROG, reference-offset governor.

with $\gamma_i \in [0; 1]$ is the fault magnitude for an actuator $i \in \{1, \ldots, m\}$ and m denotes the number of actuators.
The system state representation is

$$\begin{aligned} x(t+1) &= (A - B_f K_f)x(t) + B_f K_z^f z(t) + G_d d(t) \\ &= (A - BK_f + B\Gamma K_f)x(t) + \left(BK_z^f - B\Gamma K_z^f\right) z(t) + G_d d(t) \\ &= (\Phi + B\Gamma K_f)x(t) + \left(G - B\Gamma K_z^f\right) z(t) + G_d d(t) \\ &= \Phi_f x(t) + G_f z(t) + G_d d(t) \end{aligned} \tag{28}$$

where K_f and K_r^f are the reconfigured feedback and feed-forward gain matrices, and Φ_f and G_f represent the closed-loop system behavior after fault occurrence:

$$\begin{aligned} \Phi_f &= \Phi + B\Gamma K_f \\ G_f &= G - B\Gamma K_z^f \\ H_c^f &= -K_f \\ L_f &= K_z^f \end{aligned}$$

Thus, the state description of the plant becomes

$$\begin{cases} x(t+1) = \Phi_f x(t) + G_f z(t) + G_d d(t) \\ y(t) = H_y x(t) \\ c(t) = H_c^f x(t) + L_f z(t) + L_d d(t) \end{cases} \tag{29}$$

Figure 5 shows the proposed FTC system scheme with reconfiguration action on the feedback and feed-forward gain matrices and the ROG unit. It is assumed that instant results are obtained via fault detection and diagnosis scheme.

4.3. Reference-offset governor design in post-fault system

We propose here an extension of the ROG principle ([19]) in the faulty case (Figure 5). The calculation of the new reference z depends on the new faulty system behavior and states. The system constraints, also, may be affected by the fault occurrence. However, the following two assumptions should be still valid :

B.1 Φ_f is a stable matrix;

B.2 The system (29) is offset free with respect to $g(t)$, that is, $H_y(I_n - \Phi_f)^{-1} G_g^f = I_p$.

The solution of the cost function (21) exists:

$$z(t) := arg \min_{z \in \mathcal{V}_f(x(t))} J(x(t), z(t), r) \tag{30}$$

DOI: 10.1002/rnc

with $\mathcal{V}_f(x(t))$ as the set of the disturbance-free virtual evolution of the constraint vector $\bar{c}_f(k, x(t), z)$ after fault occurrence

$$\mathcal{V}_f(x(t)) = \left\{ z \in \mathcal{W}_\delta^f : \bar{c}_f(k, x(t), z) \in \mathcal{C}_k^f, \forall k \in \mathcal{Z}_+ \right\} \tag{31}$$

where $\bar{c}_f(k, x(t), z)$ is given by

$$\bar{c}_f(k, x(t), z) = H_c^f \left(\Phi_f^k x(t) + \sum_{i=0}^{k-1} \Phi_f^{k-i-1} G_f z \right) + L_f z \tag{32}$$

and the two sets, $\mathcal{W}_\delta^f$ and $\mathcal{C}_f^\delta$, are given by

$$\mathcal{W}_\delta^f := \left\{ z \in \mathcal{R}^{p+m} : \bar{c}_z \in \mathcal{C}_f^\delta \right\} \tag{33}$$

$$\mathcal{C}_f^\delta := \mathcal{C}_\infty^f \sim \mathcal{B}_\delta \tag{34}$$

Note that $\mathcal{C}_\infty^f$ is constructed from recursive sets $\mathcal{C}_k^f$:

$$\mathcal{C}_\infty^f := \bigcap_{k=0}^{k_0^f} \mathcal{C}_k^f \tag{35}$$

where the sets $\mathcal{C}_k^f$ are defined from $k \in \left\{0, 1, \ldots, k_0^f\right\}$ as

$$\begin{aligned} \mathcal{C}_0^f &:= \mathcal{C}^f \sim L_d \mathcal{D} \\ &\vdots \\ \mathcal{C}_k^f &:= \mathcal{C}_{k-1}^f \sim H_c^f \Phi_f^{k-1} G_d \mathcal{D} \end{aligned} \tag{36}$$

with $\mathcal{C}^f$ as the prescribed constrained set after fault occurrence and k_0^f as the pre-calculated constant integer.

4.4. System stability analysis

Let us consider the system with ROG as described in (29), the following properties hold true.

Theorem 1 ([20]*)*
Let Φ_f be a stable matrix. Consider system (29) with the ROG selection rule (30), and let $\mathcal{V}_f(x(0))$ be non-empty. Then,

1. The minimizer in (30) uniquely exists at each $t \in \mathcal{Z}_+$ and can be obtained by solving a convex constrained optimization problem, namely, $\mathcal{V}_f(x(0)) = \mathcal{V}(x(t_f))$ as non-empty implies that $\mathcal{V}_f(x(t))$ is non-empty along the trajectories generated by the ROG command (29). Such time of fault occurrence t_f is determined by the FDD stage.
2. The set $\mathcal{V}_f(x(t)), \forall x(t) \in \mathcal{R}^n$, is finitely determined, namely, there exists an integer k_0^f such that if $\bar{c}_f(k, x(t), z) \in \mathcal{C}_k^f, k \in \left\{0, 1, \ldots, k_0^f\right\}$, then $\bar{c}_f(k, x(t), z) \in \mathcal{C}_k^f \forall k \in \mathcal{Z}_+$. Such a constraint horizon k_0^f can be determined off-line.
3. The constraints are fulfilled for all $t \in \mathcal{Z}_+$.
4. The overall system is asymptotically stable.

In particular, whenever $r(t) \equiv r$, $\lim_{t \to \infty} \theta(t) = 0_m$, and $g(t)$ converges either to r or to its best steady-state admissible approximation $\hat{r}$, with

$$\hat{z}(t) := [\hat{r} \quad 0_m]^T := arg \min_{z \in \mathcal{V}_f(x(t))} J(z(t), r) \tag{37}$$

DOI: 10.1002/rnc

Consequently, by the offset-free condition (B.2), $\lim_{t\to\infty} \bar{y}(t) = \hat{r}$, where $\bar{y}$ is the disturbance-free component of y.

5. ILLUSTRATIVE EXAMPLE

5.1. System description and model

The example of the study concerns a flight control system, based on ADMIRE model ([24] and [25]), for delta-canard configuration describing the small single-engine fighter. The controlled variables are the angle of attack, α, and the roll rate, p. The sideslip angle, β, is to be regulated to 0. The system states include, besides the manipulated variables, the pitch rate, q, and the yaw rate, r. The control surface vector contains the position of the canard wings, δ_c, the right and left elevons, δ_{re} and δ_{le}, and the rudder, δ_r.

For this considered flight case, we consider low speed, mach 0.22, and altitude 3000 m. In addition, the actuator dynamics are neglected, and the actuator position constraints are set at

$$\delta_{\min} = (-55^\circ \quad -30^\circ \quad -30^\circ \quad -30^\circ)^T$$
$$\delta_{\max} = (25^\circ \quad 30^\circ \quad 30^\circ \quad 30^\circ)^T$$

Consider the following vectors for output, state, and control variables.

$$y = (\alpha \quad \beta \quad p)^T$$
$$x = (\alpha \quad \beta \quad p \quad q \quad r)^T$$
$$\delta = (\delta_c \quad \delta_{re} \quad \delta_{le} \quad \delta_r)^T$$

The linearized model is

$$\begin{cases} x(t+1) = Ax(t) + B\delta(t) \\ y(t) = Cx(t) \end{cases} \tag{38}$$

For sampling time of 0.5 s, the discrete model is

$$A = \begin{pmatrix} 1.0214 & 0.0054 & 0.0003 & 0.4176 & -0.0013 \\ 0 & 0.6307 & 0.0821 & 0 & -0.3792 \\ 0 & -3.4485 & 0.3979 & 0 & 1.1569 \\ 1.1199 & 0.0024 & 0.0001 & 1.0374 & -0.0003 \\ 0 & 0.3802 & -0.0156 & 0 & 0.8062 \end{pmatrix}$$

$$B = \begin{pmatrix} 0.1823 & -0.1798 & -0.1795 & 0.0008 \\ 0 & -0.0639 & 0.0639 & 0.1397 \\ 0 & -1.5840 & 1.5840 & 0.2936 \\ 0.8075 & -0.6456 & -0.6456 & 0.0013 \\ 0 & -0.1005 & 0.1005 & -0.4114 \end{pmatrix}$$

$$C = \begin{pmatrix} 1 & 0 & 0 & 0 & 0 \\ 0 & 1 & 0 & 0 & 0 \\ 0 & 0 & 1 & 0 & 0 \end{pmatrix}$$

After setting Q and R of the LQ controller to

$$Q = diag(1, 2, 1, 1, 3)$$

$$R = diag(5, 20, 12, 2)$$

DOI: 10.1002/rnc

one obtains

$$K = \begin{pmatrix} 1.0610 & 0.0059 & 0.0003 & 0.6264 & -0.0012 \\ -0.9294 & 0.2306 & -0.2042 & -0.5348 & -0.1089 \\ -0.9275 & -0.2409 & 0.2037 & -0.5338 & 0.1110 \\ 0.0040 & 0.4245 & 0.1228 & 0.0021 & -1.1279 \end{pmatrix}$$

$$K_r = \begin{pmatrix} 0.8393 & -0.0049 & 0.0001 \\ -0.7818 & -0.7399 & -0.3450 \\ -0.7793 & 0.7481 & 0.3448 \\ 0.0054 & 1.9978 & -0.2161 \end{pmatrix}$$

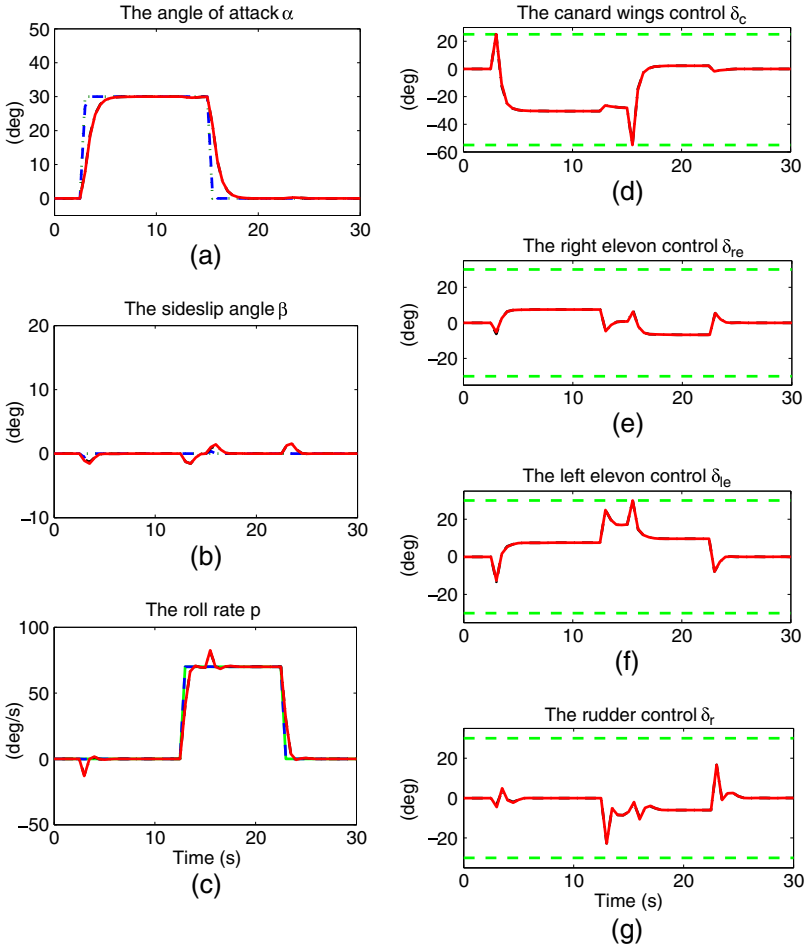

Figure 6. Fault-free system references, outputs, and control signals. (a)–(c) sub-figures: dashed-dotted line, outputs without reference-offset governor (ROG) block; continuous line, outputs with ROG block; dotted line, nominal references; dashed line, modified references. (d)–(g) sub-figures: continuous line, controls with ROG block; dashed-dotted line, controls without ROG block; dashed line, upper and lower control limits.

DOI: 10.1002/rnc

5.2. Simulation results in fault-free case

The closed-loop model of the system is

$$\Phi = \begin{pmatrix} 0.4944 & 0.0022 & -0.0000 & 0.1115 & 0.0001 \\ -0.0007 & 0.6015 & 0.0388 & -0.0004 & -0.2357 \\ -0.0041 & -2.8261 & -0.2844 & -0.0022 & 1.1397 \\ -0.9357 & -0.0096 & -0.0007 & -0.1583 & 0.0035 \\ 0.0014 & 0.6022 & -0.0060 & 0.0008 & 0.3201 \end{pmatrix}$$

and

$$G = \begin{pmatrix} 0.4335 & -0.0006 & -0.0000 & 0.1823 & -0.1798 & -0.1795 & 0.0008 \\ 0.0009 & 0.3742 & 0.0139 & 0 & -0.0639 & 0.0639 & 0.1397 \\ 0.0055 & 2.9437 & 1.0293 & 0 & -1.5840 & 1.5840 & 0.2936 \\ 1.6856 & -0.0066 & -0.0001 & 0.8075 & -0.6456 & -0.6456 & 0.0013 \\ -0.0020 & -0.6723 & 0.1582 & 0 & -0.1005 & 0.1005 & -0.4114 \end{pmatrix}$$

Figure 6 shows that the controlled outputs α, β, and p can track the nominal references, which correspond, respectively, to 30° for α in Figure 6(a), 0° for β in Figure 6(b), and 70°/s for p in Figure 6(c). Nevertheless, the ROG unit has no action here because the constraints are still respected.

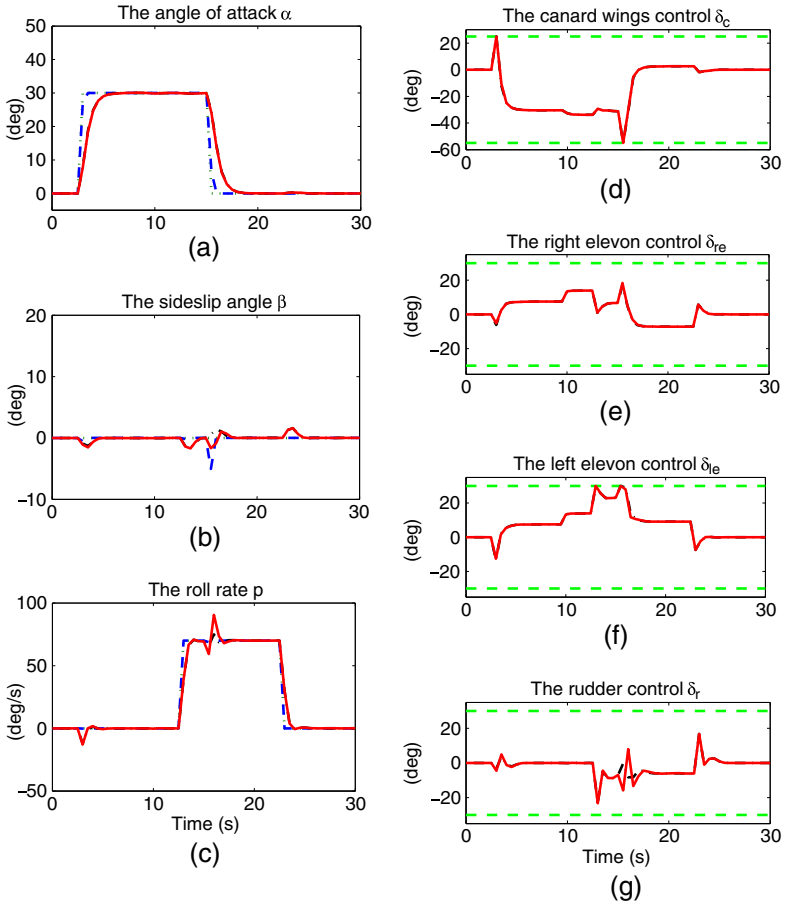

Figure 7. Faulty case system signals for scenario 1 (fault with $\gamma_1 = 0.40$). (a)–(c) sub-figures: dashed-dotted line, outputs without reference-offset governor (ROG) block; continuous line, outputs with ROG block; dotted line, nominal references; dashed line, modified references. (d)–(g) sub-figures: continuous line, controls with ROG block; dashed-dotted line, controls without ROG block; dashed line, upper and lower control limits.

DOI: 10.1002/rnc

These constraints are shown in Figure 6 ((d), (e), (f), and (g)) where the control signals of canard wings, elevons, and rudder (Figure 6(d)–(g), respectively) are still in the control bandwidths, which represented in dashed lines.

5.3. *Post-fault simulations and results*

In this case, only the fault on actuator 1, which enables the control position of the canard wings is considered. Furthermore, the fault occurs at t_f equal to 10 s. To study the effect of fault magnitude on the system behavior, we consider three fault magnitude values:

- scenario 1: Actuator 1 loses 40% of its control effectiveness at time t_f.
- scenario 2: Actuator 1 loses 75% of its control effectiveness at time t_f.
- scenario 3: Actuator 1 loses 100% of its control effectiveness at time t_f, and it is completely out of service.

The results of simulation are shown in Figure 7 for first scenario, in Figure 8 for the second scenario and in Figure 9 for the third scenario.

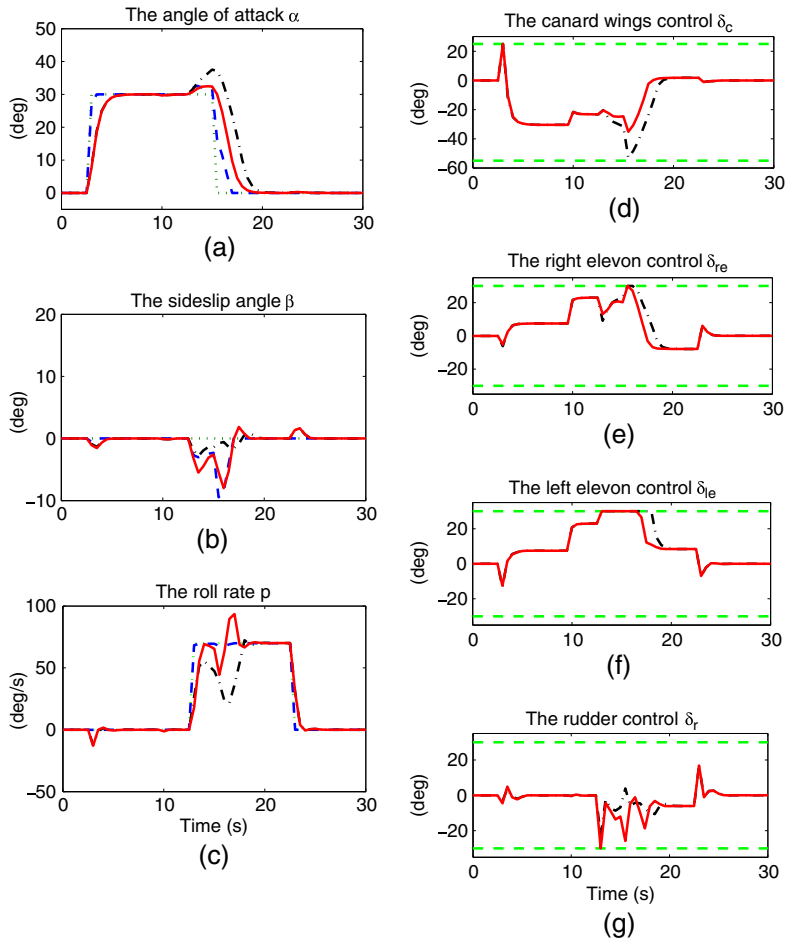

Figure 8. Faulty case system signals for scenario 2 (fault with $\gamma_1 = 0.75$). (a)–(c) sub-figures: dashed-dotted line, outputs without reference-offset governor (ROG) block; continuous line, outputs with ROG block; dotted line, nominal references; dashed line, modified references. (d)–(g) sub-figures: continuous line, controls with ROG block; dashed-dotted line, controls without ROG block; dashed line, upper and lower control limits.

DOI: 10.1002/rnc

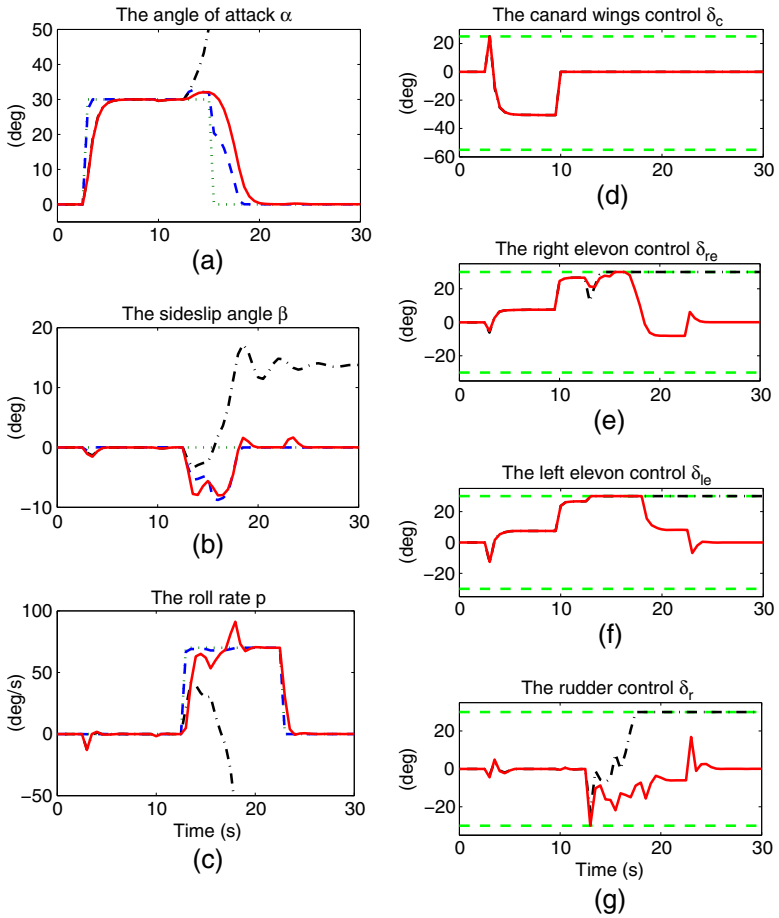

Figure 9. Faulty case system signals for scenario 3 (fault with $\gamma_1 = 1.00$). (a)–(c) sub-figures: dashed-dotted line, outputs without reference-offset governor (ROG) block; continuous line, outputs with ROG block; dotted line, nominal references; dashed line, modified references. (d)–(g) sub-figures: continuous line, controls with ROG block; dashed-dotted line, controls without ROG block; dashed line, upper and lower control limits.

Notice that for the mentioned figures (Figures 7–9) and for reason of clearance and comparison, each figure is divided into two parts : left and right. In the left part, we include the nominal references, the modified references, the system responses according to Figure 2 and those according to Figure 5. In the right part, the control signals according to Figures 2 and 5 joined by the upper and lower control limits are included.

5.4. Interpretations

For minor loss of control effectiveness in actuator 1, $\gamma_1 = 0.40$ (Figure 7), the system responses, and the control surface positions for both with and without ROG units are almost identical. In addition, the control signals are slightly changed to compensate the fault effect. However, the control signal of actuator 3 in Figure 7(f) reaches the upper limit at time 15.5 s for a short time, which induces the slight modification of the references of the sideslip angle β in Figure 7(b) and the roll rate p in Figure 7(c) to avoid such constraint violation.

In the second fault case, and for a significant loss of control effectiveness, $\gamma_1 = 0.75$ (Figure 8), the control signal of actuator 3 in Figure 8(f) reaches the upper limit at time 13 s during about 4 s. At this time, two reactions occur. For the first reconfiguration scheme, which includes only reconfigurable LQ controller without ROG unit, the limitation of control signals decreases system performance and, in the same time, increases reference tracking error especially for angle of attack

DOI: 10.1002/rnc

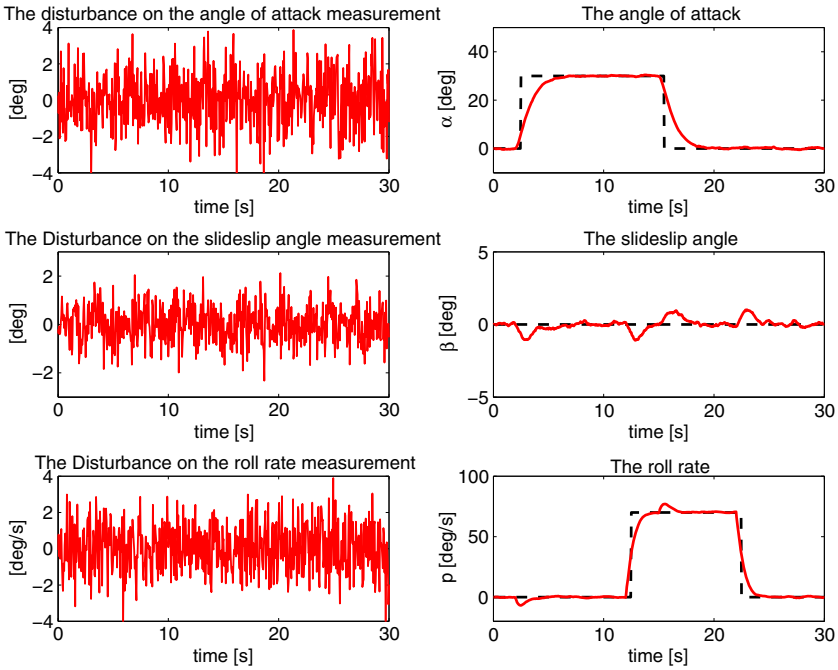

Figure 10. Output signals with disturbance consideration.

and roll rate responses in Figure 8(a) and (c), respectively. Nevertheless, in the second reconfiguration scheme where the ROG unit is associated to the LQ controller in reconfiguration scheme, the ROG unit modifies smoothly the nominal references (Figure 8(a)–(c)) to prevent the saturation of actuators (Figure 8(e) and (f)) and which reduces the reference tracking error compared with those of the previous graphs (see continuous and dotted curves in Figure 8(a)–(c)).

In the third fault case, we consider a complete loss of actuator 1, $\gamma_1 = 1.00$ (Figure 9). In this case, and after the detection of the actuator fault about 2.5 s, the actuator 3 in Figure 9(f) becomes saturated, which triggers the saturation of actuator 2 in Figure 9(e) 2 s later and actuator 4 in Figure 9(g) 5 s later, and all the system becomes instable (see dotted line curves in Figure 9(a)–(c)). On the other hand, the ROG unit makes the system stable despite the fact that the tracking error is more important. This is clearly shown by continuous line curves in Figure 9(a)–(c).

Note that only the fault of actuator 1 is treated here. Similar simulation results concerning the other actuators are omitted for reason of space.

5.5. *Robustness to disturbances*

In the example presented earlier, the disturbances have been omitted for sake of simplicity and to emphasize only on the fault effect. In this section, the proposed method has been applied in the case of persistent disturbances, $d(t)$, affecting the system. The disturbance, which is considered in this section is a Gaussian white noise:

$$d_i(t) \sim N\left(0, \sigma_i^2\right)$$

where d_i is the disturbance and $N\left(0, \sigma_i^2\right)$ is a 0-mean normal distribution with variance σ_i^2 corresponding to the ith measurement ($i = 1, \cdots, 3$).

Figures 10 and 11 show that the system exhibits quite good performances in the presence of such disturbances.

DOI: 10.1002/rnc

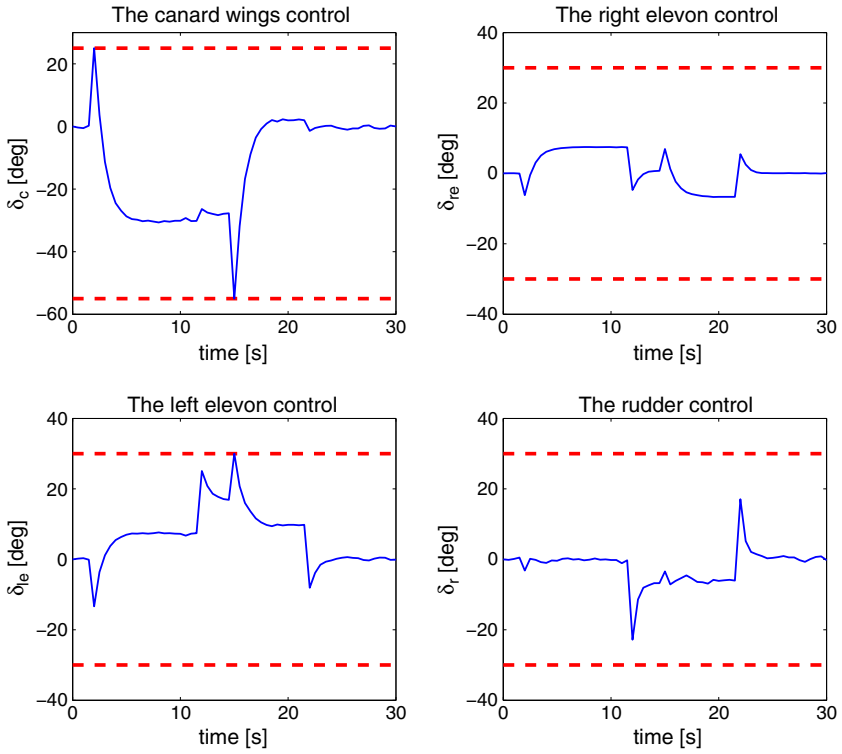

Figure 11. System control signals with disturbance consideration.

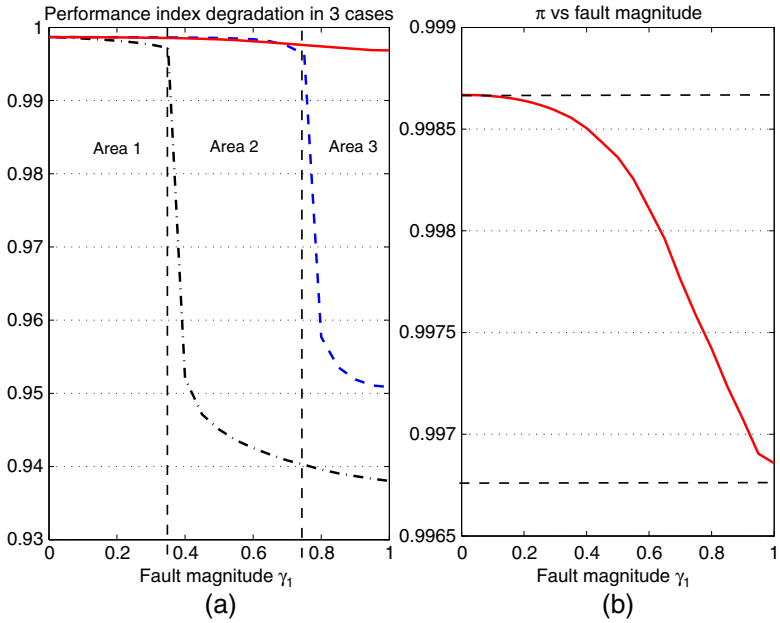

Figure 12. Performance index versus fault severity. (a) sub-figure—performance degradation in three cases: dotted line, system without reconfiguration; dashed line, only controller reconfiguration; continuous line, controller and reference-offset governor reconfiguration. (b) sub-figure—zoom in of the performance degradation index in the third case.

DOI: 10.1002/rnc

5.6. Performance evaluation

To evaluate the performance of the closed-loop system, one could use the following performance index π:

$$\pi = 1 - \frac{1}{N}\sum_{t=1}^{N}\left(\frac{\|y(t) - r(t)\|_2}{\|r(t)\|_2}\right) \tag{39}$$

where t is the sampled time and N is the number of samples. Figure 12 shows the performance index π versus the actuator 1 fault magnitude γ_1. In Figure 12(a), three operating regions could be identified as introduced in Figure 1 region 1 where γ_1 is less than 0.34, which corresponds to intrinsic controller robustnes; region 2 where γ_1 is less than 0.73, which shows the necessity of reconfiguring the system; and region 3 shows the need to degrade performance. Figure 12(b) represents the small degradation of performances on the basis of proposed scheme. In fact, the nominal performance index is 99.87% and then decreases to 99.68% in worst case, which corresponds to degradation of about 0.2%. This performance degradation is always acceptable.

6. CONCLUSION

This paper presents a new approach to fault accommodation based on ROG. The degraded ROG-based FTC modifies the references and adds an offset to the control inputs after fault occurrence to accommodate the fault with acceptable degraded performance. The goal of this ROG is to avoid actuator saturation due to fault occurrence, meanwhile reducing the degradation of performance. The simulation results are proofs that this approach improves the system performance degradation and ensures a safe and stable plant operation.

REFERENCES

1. Jiang B, Yang H, Cocquempot V. Results and perspectives on fault tolerant control for a class of hybrid systems. *International Journal of Control* 2011; **84**(2):396–411.
2. Lunze J, Richter J. Reconfigurable fault-tolerant control: A tutorial introduction. *European Journal of Control* 2008; **5**:359–386.
3. Patton R. Fault-tolerant control systems: The 1997 situation. In *The 3rd IFAC Symposium on Fault Detection, Supervision and Safety for Technical Processes* (August 1997), Hull, UK, 1997; 1033–1054.
4. Zhang Y, Jiang J. Bibliographical review on reconfigurable fault-tolerant control systems. In *The 5th IFAC Symposium on Fault Detection, Supervision and safety for Technical Processes* (9-11 June 2003), Washington, D.C., USA, 2003; 265–276.
5. Aubrun C, De Cuypere P, Sauter D. Design of a supervised control system for sludge dewatering process. *Control Engineering Practice* 2003; **11**:27–37.
6. Jiang J, Zhang Y. Accepting performance degradation in fault-tolerant control system design. *IEEE Transactions on Control Systems Technology* 2006; **14**:284–292.
7. Zhang Y, Jiang J. Fault tolerant control system design with explicit consideration of performance degradation. *IEEE Transactions on Aerospace and Electronic Systems* 2003; **39**:838–848.
8. Jiang J, Zhang Y. Graceful performance degradation in active fault tolerant control systems. In *15th Triennial World Congress of the International Federation of Automatic Control* (21-26 July 2002), Barcelona, Spain, 2002.
9. Mayne Q, Rawlings B, Rao V, Scokaert M. Constrained model predictive control: Stability and optimality. *Automatica* 2000; **36**(6):789–814.
10. Kothare MV, Morari M. Multiplier theory for stability analysis of anti-windup control systems. *Automatica* 1999; **35**:917–928.
11. Wu F, Lu B. Anti-windup control design for exponentially unstable LTI systems with actuator saturation. *Systems & Control Letters* 2004; **52**:305–322.
12. Angeli D, Casavola A, Mosca E. On feasible set-membership state estimators in constrained command governor control. *Automatica* 2001; **37**:151–156.
13. Bemporad A, Casavola A, Mosca E. Nonlinear control of constrained linear systems via predictive reference management. *IEEE Transactions on Automatic Control* 1997; **42**:340–349.
14. Boussaid B, Aubrun C, Ben Gayed K, Abdelkrim MN. FTC approach based on predictive governor. In *7th IEEE International Conference on Control and Automation* (9-11 December 2009), Chrischurch, New Zealand, 2009; 2088–2093.
15. Casavola A, Mosca E, Angeli D. Robust command governors for constrained linear systems. *IEEE Transactions on Automatic Control* 2000; **45**:2071–2077.

DOI: 10.1002/rnc

16. Gilbert E, Kalmanovsky I, Tan K. Discrete-time reference governors and the nonlinear control of systems with state and control constraints. *International Journal of Robust and Nonlinear Control* 1995; **5**:487–504.
17. Gilbert E, Tan K. Linear systems with state and control constraints: The theory and application of maximal output admissible sets. *IEEE Transactions on Automatic Control* 1991; **36**:1008–1020.
18. Kolmanovsky I, Sun J. Parameter governors for discrete-time nonlinear systems with pointwise-in-time state and control constraints. *Automatica* 2006; **42**:841–848.
19. Casavola A, Franz G, Sorbara M. Reference-offset governor approach for the supervision of constrained networked dynamical system. In *European Control Conference* (2-5 July 2007), Kos, Greece, 2007; 7–14.
20. Casavola A, Papini M, Franz G. Supervision of networked dynamical systems under coordination constraints. *IEEE Transactions on Automatic Control* 2006; **51**(3):421–43.
21. Glad T, Ljung L. *Control Theory: Multivariable and Nonlinear Methods*. Taylor & Francis, CRC Press, 2000.
22. Staroswiecki M. Actuator faults and the linear quadratic control problem. In *42th IEEE Conference on Decision and Control* (2003), Maui, Hawaii, USA, 2003; 959–965.
23. Kapasouris P, Athans M, Stein G. Design of feedback control systems for stable plants with saturating actuators. In *27th IEEE Conference on Decision and Control* (1988), Austin, Texas, USA, 1988; 469–479.
24. ADMIRE ver. 3.4h., Aerodata Model in Research Environment (ADMIRE), version 3.4h, Swedish Defence Research Agency (FOI), 2003.
25. Harkegard O, Glad S. Resolving actuator redundancy—optimal control vs. control allocation. *Automatica* 2005; **41**:137–144.

DOI: 10.1002/rnc